

1 **Effect of leaf temperature on the estimation of photosynthetic and other traits of wheat**
2 **leaves from hyperspectral reflectance**

3 **Hammad A Khan^{1,*}, Yukiko Nakamura^{1,2}, Robert T Furbank^{1,3} and John R Evans¹**

4 ¹ ARC Centre of Excellence for Translational Photosynthesis, Research School of Biology. The
5 Australian National University, Canberra, ACT 2601, Australia

6 ² Graduate School of Life Sciences, Tohoku University, Japan

7 ³ CSIRO Agriculture & Food, Canberra, ACT 2601, Australia

8 * Present address: CSIRO Agriculture & Food, Waite Campus, Glen Osmond, SA 5064,
9 Australia

10 ORCID

11 HK [0000-0001-7859-8274](https://orcid.org/0000-0001-7859-8274)

12 RTF [0000-0001-8700-6613](https://orcid.org/0000-0001-8700-6613)

13 JRE 0000-0003-1379-3532

14

15 **Abstract**

16 A growing number of leaf traits can be estimated from hyperspectral reflectance data. These
17 include structural and compositional traits, such as leaf mass per area (LMA), nitrogen and
18 chlorophyll content, but also physiological traits such as Rubisco carboxylation activity,
19 electron transport rate and respiration rate. Since physiological traits vary with leaf
20 temperature, how does this impact on predictions made from reflectance measurements?
21 We investigated this with two wheat varieties, by repeatedly measuring each leaf through a
22 sequence of temperatures imposed by varying the air temperature in a growth room. Leaf
23 temperatures ranging from 20 to 35°C did not alter the estimated Rubisco capacity
24 normalised to 25°C ($V_{\text{cmax}25}$), chlorophyll or nitrogen contents per unit leaf area. Models
25 estimating LMA and $V_{\text{cmax}25}/\text{N}$ were both slightly influenced by leaf temperature: estimated
26 LMA increased by 0.27% °C⁻¹ and $V_{\text{cmax}25}/\text{N}$ increased by 0.46% °C⁻¹. A model estimating
27 Rubisco activity closely followed variation associated with leaf temperature. Reflectance
28 spectra change with leaf temperature and therefore contain a temperature signal.

29 **Keywords:** Leaf temperature, hyperspectral reflectance, Rubisco carboxylation activity,
30 electron transport rate, leaf dry mass per area, chlorophyll content, leaf nitrogen, *Triticum*
31 *aestivum*

32 **Introduction**

33 Plant breeders continually strive to improve crop yield. For cereals, there has been a
34 recognition that future increases could benefit from improving photosynthesis (Parry *et al.*,
35 2011; Reynolds *et al.*, 2009). Crop growth is not simply related to a measurement of
36 photosynthetic rate of a particular leaf under one condition. Instead, photosynthesis

37 integrated over a day with contributions from all the leaves in the canopy drives crop
38 growth. Subsequent conversion into biomass and the partitioning into harvested grains
39 determines yield. All these processes combined pose a major challenge on how to
40 meaningfully measure photosynthesis with the goal of improving yield. However, there are
41 a few examples that have compared historical sequences of cultivars and observed
42 correlations between leaf photosynthetic rate and wheat yield (Beche *et al.*, 2014; Fischer
43 *et al.*, 1998; Gaju *et al.*, 2016; Yao *et al.*, 2019). It has also been found that radiation use
44 efficiency (above ground biomass produced per unit of intercepted photosynthetically
45 active radiation) has been increasing over time with changing wheat varieties in both the UK
46 (Shearman *et al.*, 2005) and Australia (Sadras *et al.*, 2012). Interestingly, both studies found
47 the same rate of increase ($0.012 \text{ g MJ}^{-1} \text{ y}^{-1}$).

48 It is possible to survey photosynthetic properties between wheat genotypes (Driever
49 *et al.*, 2014; Silva-Perez *et al.*, 2020), but detailed phenotyping is time-consuming which
50 limits the number of genotypes that can be sampled. A promising alternative is to predict
51 photosynthetic traits from leaf reflectance spectra, an optical signal that can provide
52 information remotely and rapidly. With appropriate calibration data measured with
53 conventional methods (e.g. gas exchange or destructive sampling), predictive models can
54 be built for a range of leaf traits. Leaf reflectance is able to predict the amount of a substance
55 e.g. leaf dry mass, water or nitrogen per unit area (e.g. Ecartot *et al.*, 2013; Serbin *et al.*,
56 2012; Sims and Gamon, 2003; Zhang and Zhou, 2019). Reflectance spectra have also been
57 shown to be able to predict physiological processes. Serbin *et al.* (2012) also derived models
58 predicting maximum Rubisco carboxylase activity (V_{cmax}) and photosynthetic electron
59 transport rate measured under a PPFD of $1800 \mu\text{mol m}^{-2} \text{ s}^{-1}$ and high CO_2 (J_{1800}) from
60 hyperspectral reflectance measured on leaves of *Populus tremuloides* and *P. deltoides*.

61 Physiological processes vary with temperature and this has been used in several
62 studies to broaden the range in parameter values when establishing PLSR models. A single
63 model for V_{cmax} was developed from reflectance spectra measured on *P. tremuloides* and *P.*
64 *deltoides*, with leaf temperatures varying from 20 to 30°C (Serbin *et al.*, 2012).
65 Hyperspectral reflectance has successfully been used to predict V_{cmax} for *Glycine max*
66 measured between 26 and 34°C (Ainsworth *et al.*, 2014) and for *Nicotiana tabacum*
67 (Meacham-Hensold *et al.*, 2019) and *Zea mays* (Yendrek *et al.*, 2017) measured at various
68 temperatures in the field.

69 Models for estimating traits from leaf reflectance could consist of two components.
70 Firstly, a component that estimated the amount of a substance that was insensitive to
71 temperature. Secondly, a component that detected leaf temperature. A combination of
72 these two components could capture a trait that varied with temperature, such as V_{cmax} .
73 With Rubisco being such a major constituent of leaf protein, a reflectance model could arise
74 from a signal associated with leaf protein or nitrogen, as argued by Dechant *et al.* (2017).
75 V_{cmax} can then be obtained by knowing the kinetic properties of Rubisco and leaf
76 temperature. Changing leaf temperature would alter V_{cmax} but not Rubisco content.
77 However, Serbin *et al.* (2012) successfully predicted V_{cmax} with variation in leaf temperature,
78 demonstrating that it was possible to derive a model that captured both the amount of

79 Rubisco (or indirectly from protein or N) together with its activity. In order for a reflectance
80 model to robustly deal with variation in leaf temperature, training data would need to be
81 collected at different leaf temperatures. While the Rubisco models derived by Dechant et
82 al. (2017) and Serbin et al. (2012) could differ because they are based on different species,
83 they could also differ in the amount of variation in leaf temperature present in the training
84 data. In contrast to gas exchange measurements, where leaf temperature is measured
85 directly to enable the calculation of stomatal conductance, leaf temperature is not generally
86 measured directly during the collection of hyperspectral reflectance. Consequently, it is
87 unclear how leaf temperature might be captured by the models or how temperature might
88 affect the estimation of leaf traits from hyperspectral reflectance.

89 In order to be able to make useful comparisons of Rubisco capacity between plants
90 which may differ in their leaf temperature during sampling, one needs to know both V_{cmax}
91 and leaf temperature. Alternatively, one could use the temperature responses of the
92 Rubisco enzyme kinetic parameters (Bernacchi *et al.*, 2003; Silva-Pérez *et al.*, 2017) to
93 convert gas exchange estimates of V_{cmax} to a common temperature, e.g. 25°C ($V_{\text{cmax}25}$),
94 which are then used to build a model from reflectance data. This has been done for a group
95 of 37 broadleaf tree species (Dechant *et al.*, 2017), wheat (Silva-Perez *et al.*, 2018) and 21
96 tropical tree species from Panama and Brazil (Wu *et al.*, 2019). Heckmann et al. (2017) also
97 presented predictions of V_{cmax} for *Brassica*, *Moricandia* and *Z. mays* from reflectance
98 spectra, but measured only at 25°C. While Dechant et al. (2017) normalised their gas
99 exchange to 25°C, the reflectance spectra were collected at prevailing leaf temperatures. It
100 is not known whether the prediction of $V_{\text{cmax}25}$ from leaf reflectance is insensitive to the
101 temperature of the leaf during the reflectance measurement.

102 The near infrared absorption spectrum of water changes with temperature (Collins
103 1925, cited by Curcio and Petty, 1951). A linear change in the absorptivity of water with
104 temperature should influence leaf reflectance, although this does not appear to have been
105 widely reported. Two absorption features of pure water were identified by Langford et al.
106 (2001): absorptivity increased with increasing temperature at 738 and 836nm and
107 decreased at 796 and 888nm. Czarnik-Matusiewicz and Pilorz (2006) analysed the spectral
108 absorption changes of water around 1923nm and explained the temperature sensitivity in
109 terms of stretching and bending of OH bonds. Grass leaves contain between 0.7 and 0.86 g
110 water g⁻¹ fresh mass (Garnier and Laurent, 1994), so these spectral features should influence
111 leaf reflectance.

112 As it is likely that leaf temperature will vary when collecting reflectance spectra in
113 the field, our aim was to specifically assess whether leaf traits estimated from hyperspectral
114 reflectance varied with leaf temperature. We repeatedly measured the same leaf
115 sequentially through a range of temperatures for two wheat cultivars. Much of the training
116 data of Silva-Perez et al. (2018) was collected in the field where leaf temperature could not
117 always be held at 25°C, but varied between 25 and 34°C (see Supplementary Fig. S1 in (Silva-
118 Perez *et al.*, 2020). As variation in temperature may not have been well distributed between
119 samples, we hypothesized that some estimated traits could be affected by the temperature
120 of the leaf during the measurement of the reflectance spectra.

121

122 **Materials and Methods**123 *Plant material and growth conditions*

124 Experiment 1.

125 Two spring wheat genotypes (*Triticum aestivum* Kukri and Seri) were grown in a naturally lit
126 greenhouse (day/night temperatures set at 25/15 °C) at the Australian National University
127 in Canberra during Sep-Nov 2018. Three seeds were sown in well-drained 3.5-litre pots filled
128 with commercial potting mix, containing basal fertilizer Osmocote (Scotts). Pots were laid
129 out according to randomized block design with six replicates and blocks representing the
130 replications. After emergence, seedlings were thinned down to one plant per pot. Plants
131 were watered daily until the end of the experiment.

132 Temperature treatment was given in a controlled environmental chamber, with day/night
133 temperatures set at 25/15 °C and irradiance set to 500 $\mu\text{mol photons m}^{-2} \text{s}^{-1}$. All the
134 measurements were made seven days after anthesis. Plants were moved to the chamber
135 one day before the actual measurements so that plants could acclimatize to the chamber's
136 environmental conditions. The next day, measurements were made at a chamber
137 temperature of 15, 25, 35 and 15 °C, in the described sequence. After achieving the desired
138 chamber temperature, plants were acclimatized at least 1 hr before leaf reflectance and
139 MultispeQ measurements were made.

140 Experiment 2.

141 Two spring wheat genotypes (Kukri and Seri) and one triticale (Hawkeye) were grown in a
142 greenhouse with temperature set to 20/15 °C (day/night). Seeds were sown on multiple days
143 in March 2018 and each genotype was sown separately in a shallow tray filled with seed
144 raising mix. After germination, seedlings were transplanted into 5L pots filled commercial
145 potting mix, containing basal fertilizer Osmocote (Scotts). Five-six weeks after sowing, half
146 of the plants were transferred to an adjacent greenhouse room set at 32/20 °C, where they
147 grew for one-two more weeks before gas exchange measurements were made.

148 *Hyperspectral reflectance measurements (Experiment 1)*

149 Hyperspectral reflectance spectra were measured with a FieldSpec®4 (Analytical Spectral
150 Devices, Boulder, CO, USA) full range spectroradiometer (350–2500 nm) attached to a leaf
151 clip (Analytical Spectral Devices, Boulder, CO, USA) with a fibre optic cable. The leaf clip had
152 an internal calibrated light source and two external panels i.e. a white panel to calibrate the
153 instrument and a black panel used when measuring leaf reflectance. The PPFD at the leaf
154 surface delivered by the internal light source was 1190 $\mu\text{mol PAR photons m}^{-2} \text{s}^{-1}$. A mask
155 within a black circular gasket was attached to leaf clip to reduce the leaf-clip aperture to an
156 oval area (1.15 x 1.4 cm = 1.264 cm²) suitable for a wheat leaf (Silva-Perez *et al.*, 2018). For
157 each temperature, one reflectance measurement was made from the adaxial surface, close
158 to the middle of the flag leaf of each plant, by putting the leaf vertically into the leaf probe
159 as explained elsewhere (Silva-Perez *et al.*, 2018). Thus, for each leaf, four spectra were

160 measured at approximately the same place. Six replicate plants were measured for each
161 genotype.

162 To obtain the estimated trait values, leaf reflectance spectra were processed using the
163 models developed by Silva-Perez *et al.* (2018). Firstly, a 'jump' correction associated with a
164 change in the detectors at 1000 and 1800 nm was applied to the spectra. Jump corrected
165 spectra did not show discontinuities between the three detectors which are associated with
166 temperature dependent errors at the borders (Hueni and Bialek, 2017). Secondly, the traits
167 were estimated using the PLSR models for V_{cmax} , V_{cmax25} , V_{cmax25}/N , J_{1800} , N , SPAD and LMA
168 (Silva-Perez *et al.*, 2018).

169 *MultispeQ measurements (Experiment 1)*

170 Linear electron flow (LEF) and relative chlorophyll content (SPAD units) were measured
171 using a handheld MultispeQ (Beta) device linked to the PhotosynQ platform
172 (www.photosynq.org) (Kuhlgert *et al.*, 2016). LEF was estimated from the measurements of
173 quantum yield of photosystem II (ϕ_{II}) via pulse-amplitude modulation fluorometry with a
174 PPF of 1000 $\mu\text{mol photons m}^{-2} \text{s}^{-1}$. Relative chlorophyll content (SPAD units) was calculated
175 by the MultispeQ from transmittance measurements of red (650 nm) and infrared (940 nm)
176 light.

177 Note that for SPAD values estimated from reflectance in the previous section, the PLSR
178 model was trained on measurements using a SPAD-502 chlorophyll meter (Minolta Camera
179 Co., Ltd, Japan) (Silva-Perez *et al.*, 2018).

180 *Gas-exchange measurements (Experiment 2)*

181 Gas exchange was measured on the most recently fully expanded leaves with a LI-6400XT
182 Portable Photosynthesis system (LI-COR Biosciences Inc., Lincoln, NE, USA) on plants placed
183 inside a controlled environment cabinet (Thermoline Science Model-TRIL/SL). The air flow
184 rate was 500 $\mu\text{mol s}^{-1}$ with a PPF of 1800 $\mu\text{mol m}^{-2} \text{s}^{-1}$ supplied by the LED light. Gas
185 exchange was measured at leaf temperatures of 15, 25 and 35°C. At each temperature, CO₂
186 response curves were measured in 21% O₂ using inlet CO₂ concentrations of 400, 50, 100,
187 150, 250, 400, 600, 800, 1000, 400 $\mu\text{mol mol}^{-1}$. Subsequently, the air was changed to 2% O₂
188 with a CO₂ concentration in the leaf chamber of 380 $\mu\text{mol mol}^{-1}$, the flow reduced to 200
189 $\mu\text{mol s}^{-1}$ and measurement continued for 60 minutes with concurrent sampling for carbon
190 isotope discrimination to determine mesophyll conductance (Evans and von Caemmerer,
191 2013). Maximum Rubisco carboxylase activity (V_{cmax}) was calculated from CO₂ response
192 curves using kinetic constants derived from wheat (Silva-Pérez *et al.*, 2017).

193 In the C₃ photosynthesis model (Farquhar *et al.*, 1980), the temperature dependency of
194 Rubisco kinetic parameters is given by the Arrhenius function normalised to 25°C:

$$195 \quad P = P_{25} \exp \left[\frac{E_a(T-298)}{298RT} \right] \quad \text{Eqn. 1}$$

196 where P_{25} is the parameter value at 25°C, E_a is the activation energy (J mol^{-1}), T is the leaf
197 temperature (K) and R is the universal gas constant ($8.314 \text{ J K}^{-1} \text{ mol}^{-1}$). For wheat, we
198 assumed the value for E_a of 63 kJ mol^{-1} measured for V_{cmax} (Evans, 1986).

199 Statistical analysis

200 Data were subjected to analysis of variance and means were compared for significant
201 differences using Tukey's multiple comparison tests at 5% probability using the agricolae
202 package (De Mendiburu, 2016) in R (R_Core_Team, 2013).

203 Results

204 The effects of leaf temperature on the estimation of traits from leaf reflectance
205 spectra was investigated with two wheat varieties. The estimated value of $V_{\text{cmax}25}$ was not
206 affected by the leaf temperature when reflectance spectra were measured for Kukri, but
207 was 5% less at 27°C than either 20°C or 35°C for Seri (Fig. 1A). Upon returning the growth
208 cabinet to 15°C, the estimated $V_{\text{cmax}25}$ values were not significantly different from the initial
209 values for either cultivar. For each leaf, the deviation in the estimated value for $V_{\text{cmax}25}$ from
210 that obtained with the cabinet set to 25°C is shown in Fig. 1B. There was no significant trend
211 in the deviation with leaf temperature. A statistical comparison of the effects of
212 temperature treatments on estimated and measured leaf traits is given in Supplementary
213 Table 1.

214 By contrast, estimated V_{cmax} values (Experiment 1) increased nearly fourfold
215 between 20 and 35°C, consistent with an E_a of 63 kJ mol⁻¹ for the model curve (Fig. 2). Values
216 of V_{cmax} derived from gas exchange measurements for wheat grown under cool or hot
217 conditions (Experiment 2) followed the model curve but fell below it at 35°C, with the
218 deviation being greater for cool compared to hot grown plants. The temperature response
219 of V_{cmax} values derived from gas exchange measurements for plants from the hot treatment
220 are consistent with the previously published data from Silva-Perez et al. (2017).

221 Rates of electron transport, J , estimated from leaf reflectance varied little between
222 20 to 35°C (Fig. 3A). J was also measured using a MultispeQ instrument following the
223 collection of leaf reflectance spectra at each temperature (denoted LEF, Fig. 3A). This was
224 measured under a PPFD of 1000 $\mu\text{mol m}^{-2} \text{s}^{-1}$, similar to the irradiance in the growth cabinet.
225 As it was collected rapidly, it does not represent the steady state. LEF was similar between
226 20 and 30°C, then declined slightly at 35°C. J_{1800} derived from gas exchange measurements
227 increased by 30% between 15 and 25°C and then plateaued (Fig. 3B). The temperature
228 responses of J_{1800} obtained from Experiment 2 in this study were comparable to the
229 previously published data from Silva-Perez et al. (2017). Growth temperature shifted the
230 temperature response of J_{1800} . For plants grown under hot conditions, J_{1800} was less than
231 that from plants grown under cool conditions when measured at 15°C but greater at 35°C,
232 suggesting that there was some acclimation to the growth temperature.

233 Estimated values of chlorophyll content were insensitive to the leaf temperature
234 when reflectance spectra were measured (Fig. 4, Supplementary Table 1). There was no
235 trend in the deviations of the estimated SPAD value with leaf temperature (Fig. 4B). A similar
236 result was observed for chlorophyll content estimated with the MultispeQ (Fig. 4A),
237 although the absolute values obtained with the MultispeQ were about 20% greater than
238 that estimated from reflectance. Note that two different types of instrument were used to

239 obtain these SPAD values, but direct comparisons between the MultispeQ and SPAD-502
240 meter have not been made on the same leaf. Estimated values for three other leaf traits,
241 LMA, nitrogen content per unit leaf area and Rubisco carboxylation capacity normalised to
242 25 °C per unit leaf nitrogen ($V_{\text{cmax}25}/N$), together with the deviation of the estimates from
243 the value estimated at 25 °C are presented in Fig. 5. For both LMA and $V_{\text{cmax}25}/N$, the
244 estimated values increased slightly with increasing leaf temperature (0.27 and 0.46% °C⁻¹,
245 respectively), but estimated nitrogen content was independent of leaf temperature
246 (Supplementary Table 1).

247 The spectral response of correlations between single wavelength reflectance values
248 and leaf temperature is shown together with the reflectance spectrum (Fig. 6A). Clear
249 correlations were observed on the long wavelength shoulders of the two water absorption
250 bands with peaks at 1531 and 2038nm and a third peak in the red edge at 720nm. The
251 difference between reflectance spectra measured at 35 and 20 °C is shown for the two
252 genotypes in Fig. 6B. Pronounced differences between genotypes were apparent between
253 700 and 1300 nm, but they share similar features around the 1450 and 1950 water
254 absorption wavebands. The temperature sensitive change in absorptivity of water around
255 1923 nm (Czarnik-Matusiewicz and Pilorz, 2006) is also shown as this is likely to contribute
256 to the changes in leaf reflectance. Four wavelengths (697, 1400, 1507 and 1531 nm) were
257 identified that could be combined to predict leaf temperature (Fig. 6). By sequentially adding
258 weighted reflectance values, we were able to estimate leaf temperature for both genotypes
259 remarkably well (Fig. 7).

260 Discussion

261 Leaf hyperspectral reflectance has potential as a signal that can be used for high-
262 throughput phenotyping of photosynthetic traits at the leaf and canopy scale. The spectra
263 contain a wealth of information, but the challenge is to uncover it. The variety of traits that
264 can be successfully estimated from reflectance spectra can be divided into two categories:
265 1. Constituents (e.g. dry mass, nitrogen), 2. Physiological traits (e.g. V_{cmax}). Short term
266 variation in leaf temperature will alter the value for category 2 traits but not those in
267 category 1. The results reported here for wheat measured at three temperatures were not
268 sufficient to develop new PLSR models. Rather, they were intended to test the impact of leaf
269 temperature on the estimation of several traits in each category using previously established
270 models (Silva-Perez *et al.*, 2018). Leaf temperature clearly altered the reflectance spectra
271 from a given leaf. However, the extent to which trait values estimated from reflectance
272 models are influenced by the temperature of the leaf when spectra are measured is not
273 known for most models with the exception of V_{cmax} and J. Robustly capturing the impact of
274 temperature in models estimating traits from reflectance spectra presumably requires
275 training data collected across a variety of leaf temperatures.

276 *Parameters independent of temperature*

277 A leaf structural property that has been widely reported is leaf dry mass per unit leaf
278 area as it is easy to measure and relates to lifespan and other traits (Chavana-Bryant *et al.*,
279 2017; Wright *et al.*, 2004). Robust predictions of LMA can be made from hyperspectral

280 reflectance data (Ecarnot *et al.*, 2013; Serbin *et al.*, 2012; Silva-Perez *et al.*, 2018). As LMA is
281 a leaf property that would not change in response to short term changes in temperature,
282 models predicting LMA from hyperspectral reflectance should also be insensitive to the
283 temperature of the leaf during measurement. However, a small effect of temperature was
284 observed for estimated LMA (Fig. 5B, Supplementary Table 1). Training data collected in the
285 field that was used to generate the PLSR models included spectra measured with leaf
286 temperatures ranging between 25 and 34°C. As temperature was not distributed randomly
287 with respect to LMA throughout the training set, this could explain why the PLSR model for
288 LMA was unable to completely compensate for variable leaf temperature.

289 Estimated nitrogen and chlorophyll contents per unit leaf area were both
290 independent of the leaf temperature when reflectance spectra were measured (Figs. 4B,
291 5D). The amount of Rubisco is unlikely to vary significantly during short term changes in leaf
292 temperature, whereas the carboxylase activity is strongly temperature dependent (Badger
293 and Collatz, 1977; Bernacchi *et al.*, 2001; Sharwood *et al.*, 2016). Therefore, models using
294 reflectance to predict Rubisco content or activity normalised to a fixed temperature should
295 be independent of leaf temperature. While this was true for $V_{\text{cmax}25}$ (Fig. 1A), estimated
296 $V_{\text{cmax}25}/N$ increased slightly with increasing temperature (Fig. 5F).

297 The estimation of N, chlorophyll and $V_{\text{cmax}25}$ were each found to be unaffected by the
298 temperature of the leaf at the time reflectance was measured. However, two out of five
299 estimated parameters that were derived from the same training data and that theoretically
300 should be independent of temperature (LMA and $V_{\text{cmax}25}/N$), were found to be slightly
301 affected by leaf temperature.

302 *Parameters that vary with temperature*

303 Enzyme activities vary with temperature. For Rubisco, the temperature response of
304 V_{cmax} can be described by the Arrhenius equation through the energy of activation term E_a
305 (Equation 1). V_{cmax} can be derived from gas exchange measurements by assuming other
306 kinetic parameters of Rubisco which also vary according to Eq. 1. As there are few species
307 for which a complete set of Rubisco kinetic parameters are known, values from tobacco
308 (Bernacchi *et al.*, 2002; Bernacchi *et al.*, 2001; Sharkey *et al.*, 2007) are often assumed. In
309 some cases, a subset of temperature kinetic values have been derived from gas exchange
310 measurements (Kattge and Knorr, 2007; Serbin *et al.*, 2015; Silva-Pérez *et al.*, 2017).
311 Models estimating V_{cmax} from reflectance have been able to capture the effect of leaf
312 temperature for poplar, soybean and wheat (Ainsworth *et al.*, 2014; Serbin *et al.*, 2012;
313 Silva-Perez *et al.*, 2018), as shown in Fig. 2.

314 Reflectance spectra have also been used to estimate the rate of electron transport.
315 For poplar, J_{1800} derived from gas exchange measured at temperatures ranging from 20 to
316 30°C were successfully used to train a reflectance model (Serbin *et al.*, 2012). Reflectance
317 models estimating J_{1800} have also been established for wheat (Silva-Perez *et al.*, 2018) and
318 tobacco (Fu *et al.*, 2019; Meacham-Hensold *et al.*, 2020). For wheat measured here,
319 estimated J_{1800} varied little between 20 and 35°C (Fig. 3A) whereas LEF obtained from the
320 MultispeQ and J_{1800} derived from gas exchange did vary somewhat over that temperature

321 range. Since the temperature dependence of J_{1800} (Fig. 3B) is less pronounced than that of
322 V_{cmax} (Fig. 2) and the response varies as plants acclimate to different growth temperatures
323 (Fig. 3B, Bernacchi *et al.*, 2003; June *et al.*, 2004), the wheat J_{1800} data provides a less clear
324 validation case for the model capturing a temperature response.

325 Temperature affects the absorption of infrared light by water and also changes the
326 reflectance spectra of leaves (Fig. 6B). Based on our reflectance spectra collected at different
327 leaf temperatures, we were able to estimate leaf temperature (r^2 0.91) using just four
328 wavelengths (Fig. 7). A comparison of the difference between the models predicting V_{cmax}
329 and $V_{\text{cmax}25}$ (Silva-Perez *et al.*, 2018) did not reveal any similarity to the difference spectra in
330 Fig. 6B. It is unlikely that this equation has general application as it arose from only two
331 genotypes measured under one environment and it is known that the power and generality
332 of models predicting dark respiration (Coast *et al.*, 2019) and $V_{\text{cmax}25}$ (Wu *et al.*, 2019)
333 improved as the diversity of calibration data increased. However, the fact that leaf
334 temperature can be extracted from reflectance spectra could explain how models can
335 estimate reaction rates from reflectance.

336 **Conclusion**

337 Leaf temperature varying between 20 to 35°C during the measurement of leaf
338 reflectance did not affect estimated values of $V_{\text{cmax}25}$, chlorophyll and nitrogen contents per
339 unit area, but estimated values of LMA and $V_{\text{cmax}25}/\text{N}$ both increased slightly with increasing
340 leaf temperature. As it was possible to estimate leaf temperature from reflectance spectra,
341 this may explain how models that estimate rates that vary with temperature (V_{cmax} , J , dark
342 respiration) could arise if they are trained with data obtained across a range of leaf
343 temperatures. Traits that showed unexpected responses to temperature (LMA, $V_{\text{cmax}25}/\text{N}$)
344 may have arisen from unbalanced temperature variation within the training data. Therefore,
345 models estimating traits from reflectance spectra collected at different temperatures should
346 be tested using multiple measurements from each leaf covering a range of temperatures.
347 Reflectance appears to have the potential to predict leaf temperature, but to construct a
348 robust model would require calibration with a broader set of experiments.

349 **Acknowledgements**

350 This work was made possible by funding from the GRDC through grant ANU00025, which is
351 part of IWYP60 Using next generation approaches to exploit phenotypic variation in
352 photosynthetic efficiency to increase wheat yield, financial support from the Australian
353 Government through the Australian Research Council Centre of Excellence for Translational
354 Photosynthesis (CE140100015), and a Cooperative Laboratory Study Program grant to YN.

355 **Supplementary material**

356 Supplementary Table S1. Effects of leaf temperature on leaf physiological traits

357

Supplementary Table S1. Effects of leaf temperature on parameters measured with the MultispeQ (leaf temperature, linear electron flow (LEF), relative chlorophyll) or estimated from leaf hyperspectral reflectance ($V_{\text{cmax}25}$, J_{1800} , chlorophyll content, LMA, nitrogen content, $V_{\text{cmax}25}/N$) in leaves of two wheat genotypes exposed to a sequence of ambient air temperatures i.e. 15, 25, 35 and 15 °C, in a growth chamber (Experiment 1). For each cultivar, the mean \pm SE was calculated from measurements of one flag leaf from each of six different plants. Four sequential measurements were made on each leaf, seven days after anthesis.

Genotype	Ambient Air Temperature	Parameters measured with the MultispeQ			Parameters estimated from leaf hyperspectral reflectance					
		Leaf Temperature (°C)	LEF ($\mu\text{mol e}^- \text{m}^{-2} \text{s}^{-1}$)	Relative Chlorophyll (SPAD units)	$V_{\text{cmax}25}$ ($\mu\text{mol CO}_2 \text{m}^{-2} \text{s}^{-1}$)	J_{1800} ($\mu\text{mol e}^- \text{m}^{-2} \text{s}^{-1}$)	Relative Chlorophyll (SPAD units)	LMA (g m^{-2})	Nitrogen content (g m^{-2})	$V_{\text{cmax}25}/N$ ($\mu\text{mol CO}_2 \text{s}^{-1} \text{g}^{-1} (\text{N})$)
Kukri	15 °C	19.6 \pm 0.4	142.9 \pm 7.0	59.8 \pm 0.7	162.5 ^a \pm 1.7	196.2 ^{ab} \pm 3.6	51.8 ^{ab} \pm 0.6	54.0 \pm 1.2	2.81 \pm 0.07	59.6 ^b \pm 1.2
	25 °C	26.2 \pm 0.2	145.2 \pm 9.2	59.9 \pm 1.0	154.2 ^b \pm 1.8	184.9 ^b \pm 3.7	52.6 ^a \pm 0.4	57.4 \pm 0.8	2.90 \pm 0.05	59.7 ^b \pm 0.9
	35 °C	33.4 \pm 0.3	127.0 \pm 4.3	60.6 \pm 0.6	161.3 ^a \pm 2.2	196.3 ^{ab} \pm 4.5	50.8 ^b \pm 0.4	56.3 \pm 1.1	2.82 \pm 0.06	64.1 ^a \pm 0.6
	15 °C	19.5 \pm 0.3	145.4 \pm 8.1	59.2 \pm 1.0	165.2 ^a \pm 2.6	203.8 ^a \pm 5.0	52.7 ^a \pm 0.3	55.7 \pm 1.1	2.89 \pm 0.05	60.6 ^b \pm 1.0
	LSD (5%)		n.s.	n.s.	6.2 ^{**}	12.5 [*]	1.3 [*]	n.s.	n.s.	2.8 [*]
Seri	15 °C	19.7 \pm 0.3	144.2 ^a \pm 5.2	62.7 \pm 0.8	173.9 \pm 2.4	209.2 \pm 4.0	53.7 \pm 0.4	56.9 ^b \pm 0.7	3.05 \pm 0.05	60.1 ^b \pm 0.8
	25 °C	27.3 \pm 0.1	148.6 ^a \pm 6.1	63.3 \pm 0.8	169.5 \pm 2.2	203.5 \pm 3.7	53.8 \pm 0.2	58.5 ^{ab} \pm 0.6	3.08 \pm 0.05	61.0 ^b \pm 0.7
	35 °C	34.9 \pm 0.4	124.9 ^b \pm 3.2	64.5 \pm 0.8	169.4 \pm 2.2	203.7 \pm 4.3	53.5 \pm 0.4	60.4 ^a \pm 0.7	3.05 \pm 0.05	65.7 ^a \pm 0.7
	15 °C	19.6 \pm 0.2	145.1 ^a \pm 6.5	62.8 \pm 0.7	168.4 \pm 2.2	208.5 \pm 3.7	53.0 \pm 0.3	57.9 ^b \pm 0.9	2.96 \pm 0.04	61.5 ^b \pm 0.5
	LSD (5%)		15.9 [*]	n.s.	n.s.	n.s.	n.s.	n.s.	2.1 [*]	n.s.

*** = $P < 0.001$, ** = $P < 0.01$, * = $P < 0.05$, n.s. = non-significant

Figures

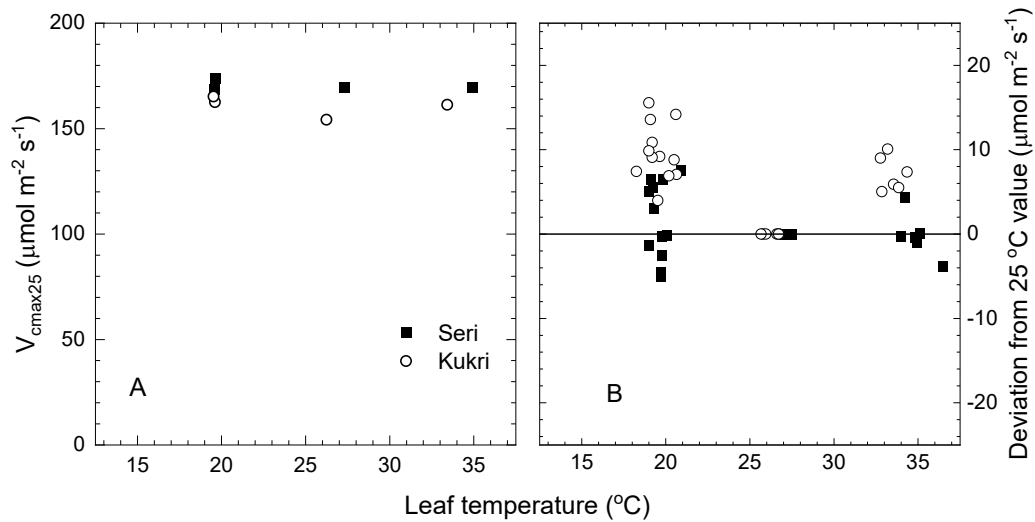


Figure 1. Effects of leaf temperature on Rubisco activity in wheat. A. The maximum rate of carboxylation by Rubisco normalised to 25 °C (V_{cmax25}) estimated from leaf hyperspectral reflectance measurements at different leaf temperatures. Seven days after anthesis, two wheat genotypes were exposed to a sequence of ambient air temperatures i.e. 15, 25, 35 and 15 °C, in a growth chamber (Experiment 1). Symbols represent the mean \pm SE of six different leaves from six different plants. B. Deviation in estimated V_{cmax25} from the value estimated at 25 ° for each leaf. There was no significant trend with the temperature of the leaf during the reflectance measurement ($P > 0.05$).

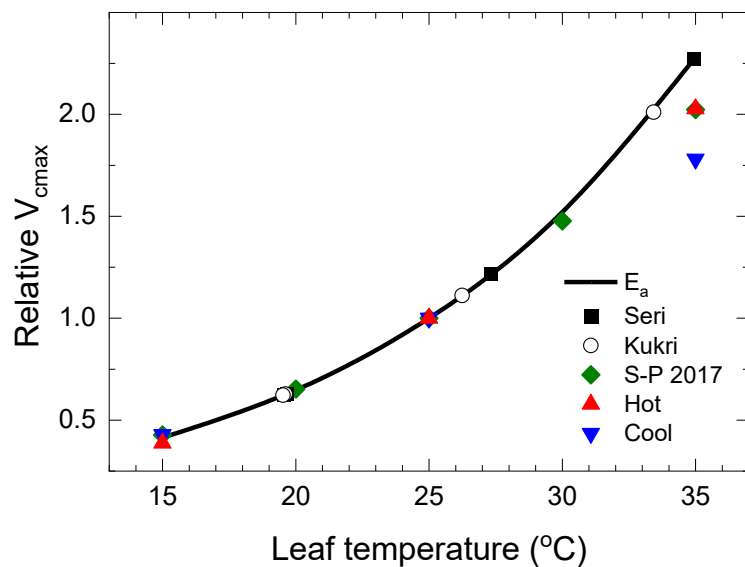


Figure 2. Temperature response of V_{cmax} normalised to 1 at 25 °C. The curve is modelled with an E_a of 63 kJ mol⁻¹. V_{cmax} estimated from leaf reflectance measurements for Seri and Kukri in experiment 1, or derived from gas exchange measurements from plants grown under hot (20/15 °C) or cool (32/20 °C) conditions (Experiment 2), or from Silva-Perez et al. (2017).

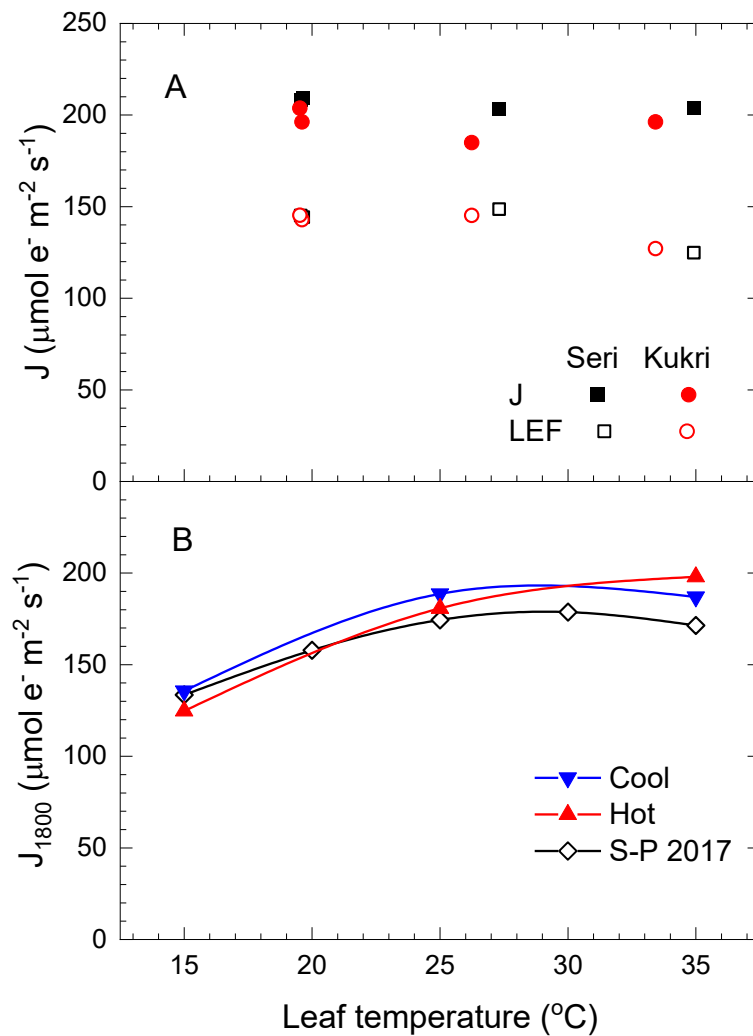


Figure 3. Effects of leaf temperature on electron transport rate in wheat. A. Rate of electron transport (J) estimated from leaf reflectance under a PPFD of $1800 \mu\text{mol m}^{-2} \text{s}^{-1}$ (solid symbols) and linear electron flow (LEF) measured using the MultispeQ under a PPFD of $1000 \mu\text{mol m}^{-2} \text{s}^{-1}$ (open symbols) at each leaf temperature. Seven days after anthesis, two wheat genotypes were exposed to a sequence of ambient air temperatures i.e. 15, 25, 35 and 15 $^{\circ}\text{C}$, in a growth chamber (Experiment 1). Symbols represent the mean \pm SE of six different leaves from six different plants. B. Rates of electron transport calculated from gas exchange measurements made under a PPFD of $1800 \mu\text{mol m}^{-2} \text{s}^{-1}$ from plants grown under cool (20/15 $^{\circ}\text{C}$) or hot (32/20 $^{\circ}\text{C}$) conditions (Experiment 2), or from Silva Perez et al. (2017).

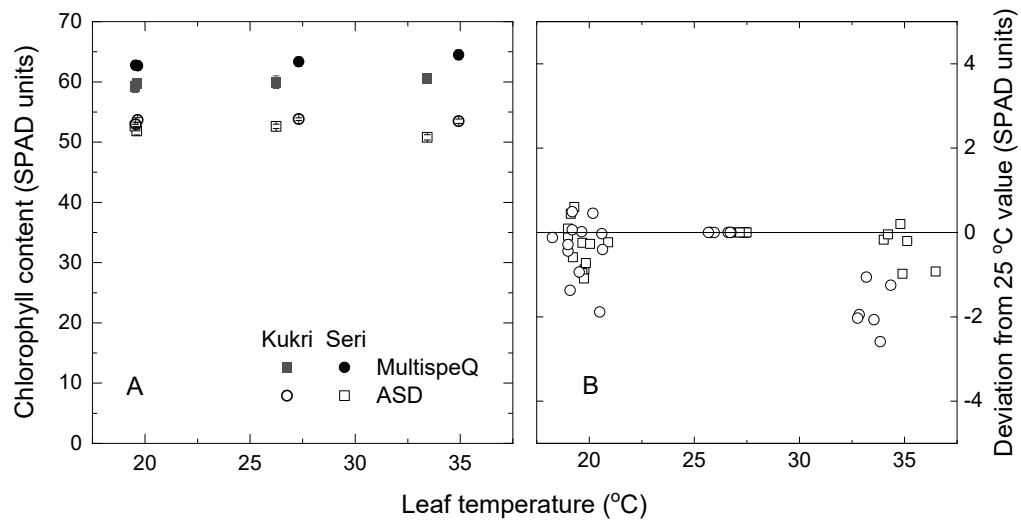


Figure 4. Effects of leaf temperature on estimated chlorophyll content (SPAD units) in wheat. Seven days after anthesis, two wheat genotypes were exposed to a sequence of ambient air temperatures i.e. 15, 25, 35 and 15 °C, in a growth chamber (Experiment 1). A. Symbols represent the mean \pm SE of six different leaves from six different plants. Leaf chlorophyll content was estimated using two different devices i.e. direct measurements with a MultispeQ or estimated from leaf hyperspectral reflectance measurements made with an ASD FieldSpec Spectroradiometer. B. Deviation in estimated SPAD from the value estimated at 25 °C for each leaf. There was no significant trend with the temperature of the leaf during the reflectance measurement ($P > 0.05$).

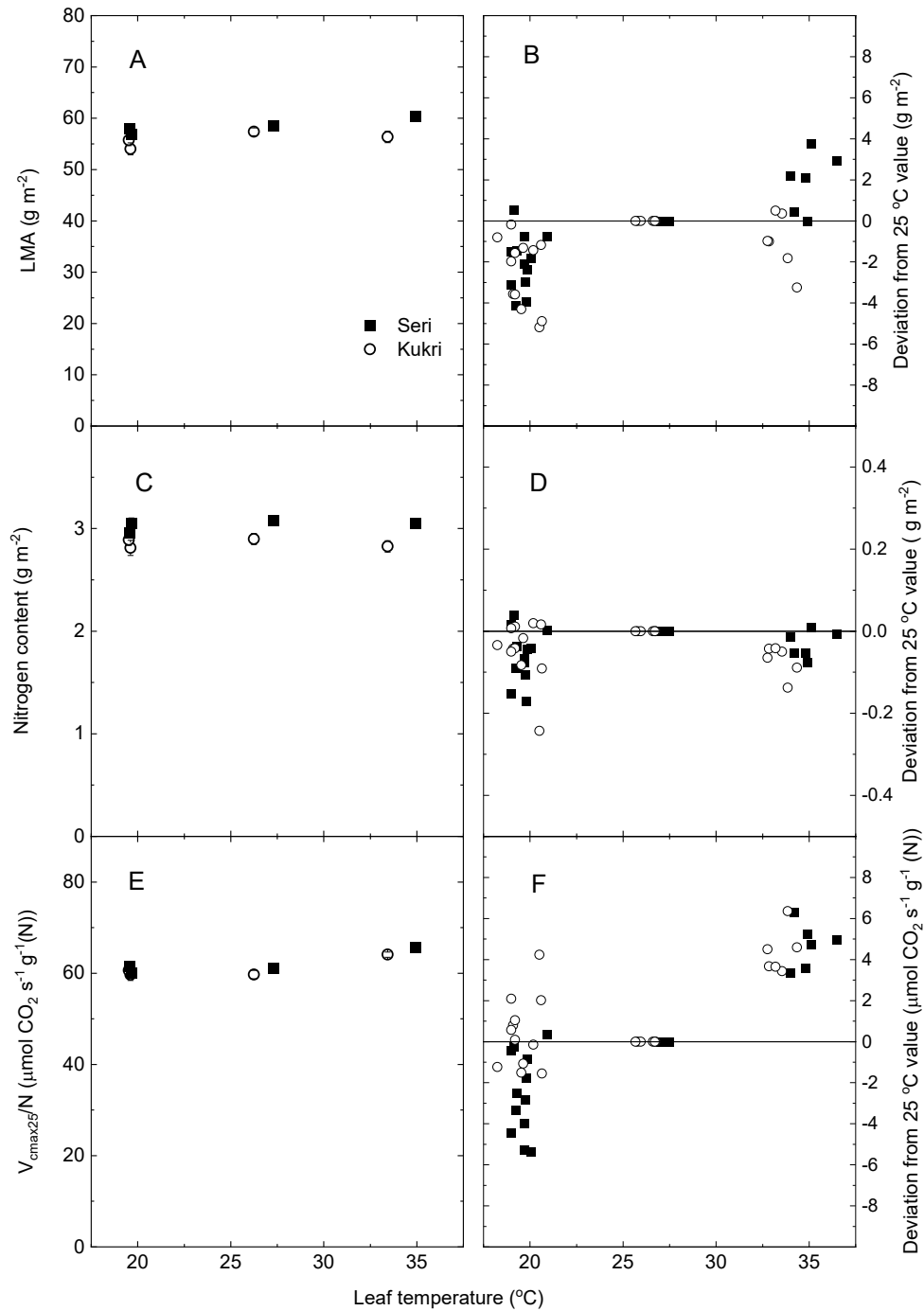


Figure 5. Effects of leaf temperature on parameters estimated from leaf hyperspectral reflectance in wheat. Seven days after anthesis, two wheat genotypes were exposed to a sequence of ambient air temperatures i.e. 15, 25, 35 and 15 °C, in a growth chamber (Experiment 1). Symbols in A, C and E represent the mean \pm SE of six different leaves from six different plants. A. Leaf dry mass per unit leaf area (LMA). B. Deviation in estimated LMA from the value estimated at 25 ° for each leaf. There was a significant positive trend with the temperature of the leaf during the reflectance measurement ($P < 0.05$) $LMA = 0.20 (\pm 0.04) \times$

T - 6.0 (\pm 0.9). C. Nitrogen content per unit leaf area. D. Deviation in estimated nitrogen content per unit leaf area from the value estimated at 25 ° for each leaf. There was no significant trend with the temperature of the leaf during the reflectance measurement ($P > 0.05$). E. Rubisco carboxylation capacity normalised to 25 °C per unit leaf nitrogen (V_{cmax25}/N). F. Deviation in estimated V_{cmax25}/N from the value estimated at 25 ° for each leaf. There was a significant positive trend with the temperature of the leaf during the reflectance measurement ($P < 0.05$) $V_{cmax25}/N = 0.36 (\pm 0.05) \times T - 8.5 (\pm 1.1)$.

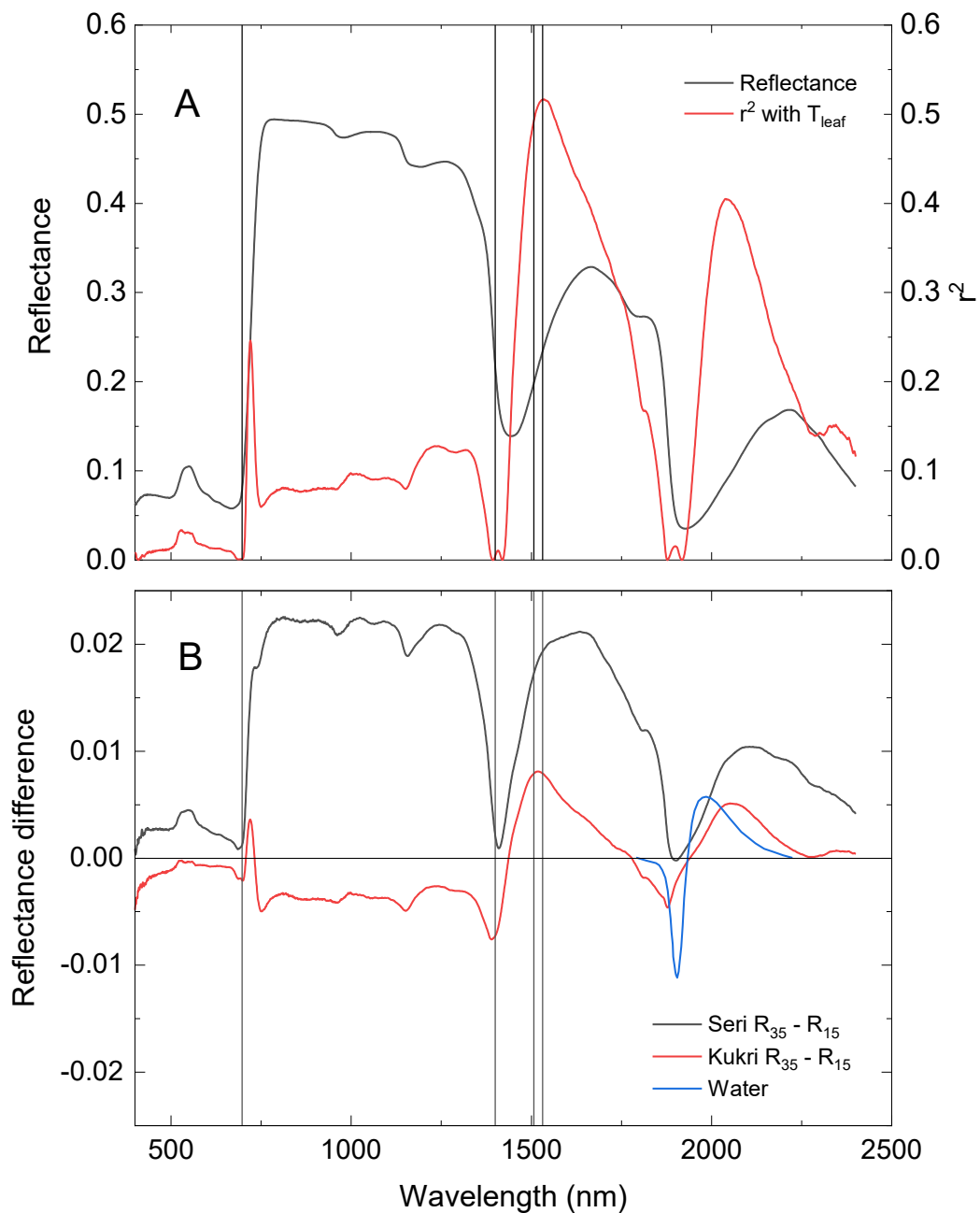


Figure 6. Effects of leaf temperature on the reflectance spectrum from a wheat leaf. A. Reflectance measured at 27°C (black line), together with the spectral response of the correlation coefficient between leaf temperature and leaf reflectance (red line). The four wavelengths used to predict leaf temperature are shown (vertical black lines, 697, 1400, 1507, and 1531 nm). B. Differences between spectra measured at 35°C and 20°C, showing averages of 6 leaves for both Seri and Kukri. Also shown is the relative difference in the molar extinction coefficient for water measured at 20 and 80°C centred around 1934 nm (Czarnik-Matusiewicz and Pilorz, 2006).

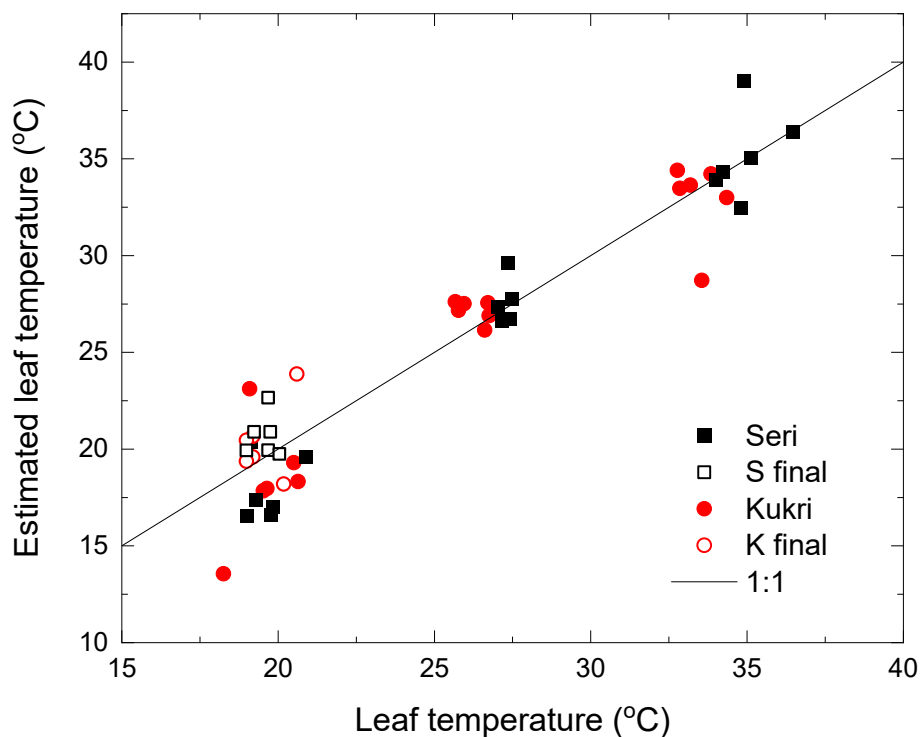


Figure 7. Relationship between leaf temperature estimated from reflectance and measured by the MultispeQ for wheat. Two wheat genotypes were exposed to a sequence of ambient air temperatures i.e. 15, 25, 35 and 15 °C which resulted in the leaf temperature increasing from 20 to 35°C (solid symbols) then decreased back to 20°C (open symbols) (Experiment 1). Measurements were made on six different leaves from six different plants. The predicted leaf temperature was calculated as: $T_{\text{leaf}} = 1071.4 R_{1531} - 945.65 R_{1400} - 176.3 R_{1507} + 196.8 R_{697}$. The fitted regression equation (not shown) was $y = 1.015x - 0.4$, $r^2 = 0.91$.

References

- Ainsworth EA, Serbin SP, Skoneczka JA, Townsend PA.** 2014. Using leaf optical properties to detect ozone effects on foliar biochemistry. *PHOTOSYNTHESIS RESEARCH* **119**, 65-76.
- Badger M, Collatz GJ.** 1977. Studies on the kinetic mechanism of ribulose-1,5-bisphosphate carboxylase and oxygenase reactions, with particular reference to the effect of temperature on kinetic parameters. *Carnegie Yearbook*, Vol. 76, 355-361.
- Beche E, Benin G, da Silva CL, Munaro LB, Marchese JA.** 2014. Genetic gain in yield and changes associated with physiological traits in Brazilian wheat during the 20th century. *European Journal of Agronomy* **61**, 49-59.
- Bernacchi CJ, Pimentel C, Long SP.** 2003. In vivo temperature response functions of parameters required to model RuBP-limited photosynthesis. *Plant, Cell & Environment* **26**, 1419-1430.
- Bernacchi CJ, Portis AR, Nakano H, von Caemmerer S, Long SP.** 2002. Temperature response of mesophyll conductance. Implications for the determination of Rubisco enzyme kinetics and for limitations to photosynthesis in vivo. *PLANT PHYSIOLOGY* **130**, 1992-1998.
- Bernacchi CJ, Singaas EL, Pimentel C, Portis AR, Long SP.** 2001. Improved temperature response functions for models of Rubisco-limited photosynthesis. *Plant, Cell & Environment* **24**, 253-259.
- Chavana-Bryant C, Malhi Y, Wu J, Asner GP, Anastasiou A, Enquist BJ, Caravasi EGC, Doughty CE, Saleska SR, Martin RE, Gerard FF.** 2017. Leaf aging of Amazonian canopy trees as revealed by spectral and physiochemical measurements. *NEW PHYTOLOGIST* **214**, 1049-1063.
- Coast O, Shah S, Ivakov A, Gaju O, Wilson PB, Posch BC, Bryant CJ, Negrini ACA, Evans JR, Condon AG, Silva-Pérez V, Reynolds MP, Pogson BJ, Millar AH, Furbank RT, Atkin OK.** 2019. Predicting dark respiration rates of wheat leaves from hyperspectral reflectance. *Plant, Cell & Environment* **42**, 2133-2150.
- Curcio JA, Petty CC.** 1951. The near infrared absorption spectrum of liquid water. *Journal of the Optical Society of America* **41**, 302-304.
- Czarnik-Matusiewicz B, Pilorz S.** 2006. Study of the temperature-dependent near-infrared spectra of water by two-dimensional correlation spectroscopy and principal components analysis. *Vibrational Spectroscopy* **40**, 235-245.
- De Mendiburu F.** 2016. Package agricolae. R package, Version 1-2.
- Dechant B, Cuntz M, Vohland M, Schulz E, Doktor D.** 2017. Estimation of photosynthesis traits from leaf reflectance spectra: Correlation to nitrogen content as the dominant mechanism. *Remote Sensing of Environment* **196**, 279-292.
- Driever SM, Lawson T, Andralojc PJ, Raines CA, Parry MAJ.** 2014. Natural variation in photosynthetic capacity, growth, and yield in 64 field-grown wheat genotypes. *JOURNAL OF EXPERIMENTAL BOTANY*.
- Ecarnot M, Compan F, Roumet P.** 2013. Assessing leaf nitrogen content and leaf mass per unit area of wheat in the field throughout plant cycle with a portable spectrometer. *Field Crops Research* **140**, 44-50.
- Evans JR.** 1986. The relationship between carbon-dioxide-limited photosynthetic rate and ribulose-1,5-bisphosphate-carboxylase content in 2 nuclear-cytoplasm substitution lines of wheat, and the coordination of ribulose-bisphosphate-carboxylation and electron-transport capacities. *PLANTA* **167**, 351-358.
- Evans JR, von Caemmerer S.** 2013. Temperature response of carbon isotope discrimination and mesophyll conductance in tobacco. *Plant Cell & Environment* **36**, 745-756.
- Farquhar GD, von Caemmerer S, Berry JA.** 1980. A biochemical model of photosynthetic CO₂ assimilation in leaves of C₃ species. *PLANTA* **149**, 78-90.
- Fischer RA, Rees D, Sayre KD, Lu ZM, Condon AG, Saavedra AL.** 1998. Wheat yield progress associated with higher stomatal conductance and photosynthetic rate, and cooler canopies. *Crop Science* **38**, 1467-1475.
- Fu P, Meacham-Hensold K, Guan KY, Bernacchi CJ.** 2019. Hyperspectral leaf reflectance as proxy for photosynthetic capacities: An ensemble approach based on multiple machine learning algorithms. *Frontiers in Plant Science* **10**.

- Gaju O, DeSilva J, Carvalho P, Hawkesford MJ, Griffiths S, Greenland A, Foulkes MJ.** 2016. Leaf photosynthesis and associations with grain yield, biomass and nitrogen-use efficiency in landraces, synthetic-derived lines and cultivars in wheat. *Field Crops Research* **193**, 1-15.
- Garnier E, Laurent G.** 1994. Leaf anatomy, specific mass and water-content in congeneric annual and perennial grass species. *NEW PHYTOLOGIST* **128**, 725-736.
- Heckmann D, Schluter U, Weber APM.** 2017. Machine learning techniques for predicting crop photosynthetic capacity from leaf reflectance spectra. *Molecular Plant* **10**, 878-890.
- Hueni A, Bialek A.** 2017. Cause, Effect, and Correction of Field Spectroradiometer Interchannel Radiometric Steps. *IEEE Journal of Selected Topics in Applied Earth Observations and Remote Sensing* **10**, 1542-1551.
- June T, Evans JR, Farquhar GD.** 2004. A simple new equation for the reversible temperature dependence of photosynthetic electron transport: a study on soybean leaf. *FUNCTIONAL PLANT BIOLOGY* **31**, 275-283.
- Kattge J, Knorr W.** 2007. Temperature acclimation in a biochemical model of photosynthesis: a reanalysis of data from 36 species. *PLANT CELL AND ENVIRONMENT* **30**, 1176-1190.
- Kuhlgert S, Austic G, Zegarac R, Osei-Bonsu I, Hoh D, Chilvers MI, Roth MG, Bi K, TerAvest D, Weebadde P, Kramer DM.** 2016. MultispeQ Beta: a tool for large-scale plant phenotyping connected to the open PhotosynQ network. *Royal Society Open Science* **3**.
- Langford VS, McKinley AJ, Quickenden TI.** 2001. Temperature dependence of the visible-near-infrared absorption spectrum of liquid water. *Journal of Physical Chemistry A* **105**, 8916-8921.
- Meacham-Hensold K, Fu P, Wu J, Serbin S, Montes CM, Ainsworth E, Guan K, Dracup E, Pederson T, Driever S, Bernacchi C.** 2020. Plot-level rapid screening for photosynthetic parameters using proximal hyperspectral imaging. *JOURNAL OF EXPERIMENTAL BOTANY* **71**, 2312-2328.
- Meacham-Hensold K, Montes CM, Wu J, Guan KY, Fu P, Ainsworth EA, Pederson T, Moore CE, Brown KL, Raines C, Bernacchi CJ.** 2019. High-throughput field phenotyping using hyperspectral reflectance and partial least squares regression (PLSR) reveals genetic modifications to photosynthetic capacity. *Remote Sensing of Environment* **231**.
- Parry MAJ, Reynolds M, Salvucci ME, Raines C, Andralojc PJ, Zhu X-G, Price GD, Condon AG, Furbank RT.** 2011. Raising yield potential of wheat. II. Increasing photosynthetic capacity and efficiency. *JOURNAL OF EXPERIMENTAL BOTANY* **62**, 453-467.
- R_Core_Team.** 2013. R: A language and environment for statistical computing. . R Foundation for Statistical Computing, Vienna, Austria.
- Reynolds M, Foulkes MJ, Slafer GA, Berry P, Parry MAJ, Snape JW, Angus WJ.** 2009. Raising yield potential in wheat. *JOURNAL OF EXPERIMENTAL BOTANY* **60**, 1899-1918.
- Sadras VO, Lawson C, Montoro A.** 2012. Photosynthetic traits in Australian wheat varieties released between 1958 and 2007. *Field Crops Research* **134**, 19-29.
- Serbin SP, Dillaway DN, Kruger EL, Townsend PA.** 2012. Leaf optical properties reflect variation in photosynthetic metabolism and its sensitivity to temperature. *JOURNAL OF EXPERIMENTAL BOTANY* **63**, 489-502.
- Serbin SP, Singh A, Desai AR, Dubois SG, Jablonski AD, Kingdon CC, Kruger EL, Townsend PA.** 2015. Remotely estimating photosynthetic capacity, and its response to temperature, in vegetation canopies using imaging spectroscopy. *Remote Sensing of Environment* **167**, 78-87.
- Sharkey TD, Bernacchi CJ, Farquhar GD, Singaas EL.** 2007. Fitting photosynthetic carbon dioxide response curves for C₃ leaves. *PLANT CELL AND ENVIRONMENT* **30**, 1035-1040.
- Sharwood RE, Ghannoum O, Kapralov MV, Gunn LH, Whitney SM.** 2016. Temperature responses of Rubisco from Paniceae grasses provide opportunities for improving C₃ photosynthesis. *Nature Plants* **2**, 16186.
- Shearman VJ, Sylvester-Bradley R, Scott RK, Foulkes MJ.** 2005. Physiological processes associated with wheat yield progress in the UK. *Crop Science* **45**, 175-185.

- Silva-Perez V, De Faveri J, Molero G, Deery DM, Condon AG, Reynolds MP, Evans JR, Furbank RT.** 2020. Genetic variation for photosynthetic capacity and efficiency in spring wheat. *JOURNAL OF EXPERIMENTAL BOTANY* **71**, 2299-2311.
- Silva-Perez V, Furbank RT, Condon AG, Evans JR.** 2017. Biochemical model of C-3 photosynthesis applied to wheat at different temperatures. *PLANT CELL AND ENVIRONMENT* **40**, 1552-1564.
- Silva-Pérez V, Furbank RT, Condon AG, Evans JR.** 2017. Biochemical model of C3 photosynthesis applied to wheat at different temperatures. *Plant, Cell & Environment* **40**, 1552-1564.
- Silva-Perez V, Molero G, Serbin SP, Condon AG, Reynolds MP, Furbank RT, Evans JR.** 2018. Hyperspectral reflectance as a tool to measure biochemical and physiological traits in wheat. *JOURNAL OF EXPERIMENTAL BOTANY* **69**, 483-496.
- Sims DA, Gamon JA.** 2003. Estimation of vegetation water content and photosynthetic tissue area from spectral reflectance: a comparison of indices based on liquid water and chlorophyll absorption features. *Remote Sensing of Environment* **84**, 526-537.
- Wright IJ, Reich PB, Westoby M, Ackerly DD, Baruch Z, Bongers F, Cavender-Bares J, Chapin T, Cornelissen JHC, Diemer M, Flexas J, Garnier E, Groom PK, Gulias J, Hikosaka K, Lamont BB, Lee T, Lee W, Lusk C, Midgley JJ, Navas M-L, Niinemets U, Oleksyn J, Osada N, Poorter H, Poot P, Prior L, Pyankov VI, Roumet C, Thomas SC, Tjoelker MG, Veneklaas EJ, Villar R.** 2004. The worldwide leaf economics spectrum. *Nature* **428**, 821-827.
- Wu J, Rogers A, Albert LP, Ely K, Prohaska N, Wolfe BT, Oliveira RC, Saleska SR, Serbin SP.** 2019. Leaf reflectance spectroscopy captures variation in carboxylation capacity across species, canopy environment and leaf age in lowland moist tropical forests. *NEW PHYTOLOGIST* **224**, 663-674.
- Yao YR, Lv LH, Zhang LH, Yao HP, Dong ZQ, Zhang JT, Ji JJ, Jia XL, Wang HJ.** 2019. Genetic gains in grain yield and physiological traits of winter wheat in Hebei Province of China, from 1964 to 2007. *Field Crops Research* **239**, 114-123.
- Yendrek CR, Tomaz T, Montes CM, Cao Y, Morse AM, Brown PJ, McIntyre LM, Leakey ADB, Ainsworth EA.** 2017. High-throughput phenotyping of maize leaf physiological and biochemical traits using hyperspectral reflectance. *PLANT PHYSIOLOGY* **173**, 614-626.
- Zhang F, Zhou G.** 2019. Estimation of vegetation water content using hyperspectral vegetation indices: a comparison of crop water indicators in response to water stress treatments for summer maize. *BMC Ecology* **19**, 1-12.